Monitoring kinetics of surface initiated atom transfer radical polymerization by quartz crystal microbalance with dissipation

Hongwei Ma[b)]
Department of Biomedical Engineering, Duke University, Durham, North Carolina 27708-0281

Marcus Textor
Department of Materials, Swiss Federal Institute of Technology, ETH, CH-8093 Zürich, Switzerland

Robert L. Clark
Department of Mechanical Engineering and Materials Science, Duke University, Durham, North Carolina 27708-0300

Ashutosh Chilkoti[a)]
Department of Biomedical Engineering, Duke University, Durham, North Carolina 27708-0281

(Received 1 February 2006; accepted 1 March 2006; published 14 April 2006)

This article reports that the kinetics of surface-initiated atom transfer radical polymerization can be quantified by the quartz crystal microbalance with dissipation (QCM-D) technique. The kinetics of *in situ* growth of poly(oligoethylene glycol methylmethacrylate) monitored on a gold-coated QCM-D sensor chip revealed that changes in the experimentally observed frequency (ΔF) and dissipation (ΔD) as a function of polymerization time were a function of the initiator density, and that the experimental response could be predicted from a continuum model. © *2006 American Vacuum Society.* [DOI: 10.1116/1.2190697]

I. INTRODUCTION

Surface initiated atom transfer radical polymerization (SI-ATRP) is a powerful technique for surface modification, because of its exquisite control of polymer chain length and surface density, and because it enables surface coatings with a range of thickness and surface densities to be synthesized *in situ* for a wide range of applications.[1–4] The independent control afforded over the polymer chain length and the surface density of the polymer chains and, hence, their configuration (e.g., mushroom, coil, or brush) are controlled by a set of multiple interacting variables such as initiator density, polymerization time and the architecture of the polymer itself—i.e., whether it is a linear polymer or a comb polymer.

An analytical challenge that hinders further development of SI-ATRP is the lack of an *in situ* method to monitor the kinetics of surface initiated polymerization (SIP) and to relate the kinetics to the interfacial architecture of the polymer film. Unlike solution polymerization, which can be monitored by retrieving samples at different time points during the course of polymerization followed by structural analysis by nuclear magnetic resonance and mass spectrometry,[5] no comparable method exists for SIP as the polymer chains are tethered to the surface. The addition of free initiator into the reaction mixture and analysis of the bulk polymer that is generated is a poor approximation of SIP as the tethered growing chains in SIP have less conformational degrees of freedom than in solution, and can also interact with the surface through secondary forces, which can alter their kinetics relative to polymerization in solution.[6]

The quartz crystal microbalance with dissipation technique (QCM-D) is ideally suited for *in situ* characterization of polymer films grown from the surface because it is a label-free, in-line technique that directly reports on the amount and viscoelastic properties of polymer films, as they grow on the surface in real-time.[7–9] A particular feature of the QCM-D technique is that frequency changes reflect not only the adsorbed mass, but also solvent molecules trapped or mechanically coupled to the adsorbed film such as structural water in swollen polymer films. Here, we show that the kinetics of SI-ATRP can be monitored *in situ* by QCM-D, and that changes in the experimentally observed frequency (ΔF) and dissipation (ΔD) can be predicted from a continuum model so that structure-property relationships that map synthesis parameters such as initiator density of the surface, time of polymerization, coating thickness, etc. can be correlated with the mass and mechanical properties of the coatings. The results reported here suggest that QCM-D is likely to be an important quantitative spectroscopic tool to characterize the interfacial architecture and mechanical properties of soft-hydrated materials.

II. METHODS

All QCM chips were cleaned by 30 min ozone plasma treatment. Mixed self-assembled monolayers (SAMs) of ω-mercaptoundecyl bromoisobutyrate (1) and 1-undecanethiol (2) were prepared by immersing gold-coated QCM chips (Q-Sense, Gothenburg, Sweden) into a 1 mM solution (total concentration) of the two thiols. QCM chips, modified with mixed SAMs of (1) and/or (2), were thoroughly rinsed with methanol to remove physisorbed thiols,

a)Author to whom correspondence should be addressed; electronic mail: chilkoti@duke.edu
b)Current address: Department of Biomedical Engineering, College of Engineering, Peking University.

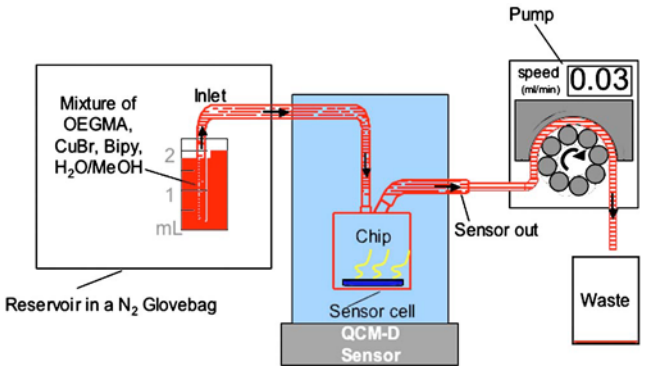

FIG. 1. Scheme of experimental setup for *in situ* SI-ATRP of OEGMA monitored in real time by QCM-D.

and placed in a Q-Sense D300 system with a window chamber (QwiC301, Q-Sense). The incomplete reactant mixture (IRM) and complete reactant mixture (CRM) were prepared as follows: IRM was obtained by mixing water (3 mL), methanol (12 mL), and the macromonomer oligo(ethylene glycol methylmethacrylate) (OEGMA) (8 g, 16.7 mmol); CRM was obtained by adding the catalyst, CuBr (50 mg, 0.3 mmol) and bipyridine (105 mg, 0.7 mmol), to IRM, which resulted in the formation of a dark red solution. Both IRM and CRM were bubbled with nitrogen for 20 min and kept under nitrogen throughout the experiment.

The SI-ATRP system that we used in this study was similar to previous reports,[10,11] and the *in situ* monitoring setup is illustrated in Fig. 1. The reactant mixture was maintained in an inert atmosphere and was coupled to the inlet of a Q-Sense D300 system (Q-Sense, Gothenburg, Sweden) through a Teflon tube, and the outlet was linked to a peristaltic pump. A typical run of SI-ATRP of OEGMA was conducted as follows: a gold-coated QCM chip, modified with a mixed SAM of (1) and/or (2) was mounted into a window chamber (QwiC301, Q-Sense), and was primed with IRM by peristaltic flow (2 mL h^{-1}) until a stable baseline was established. Next, SI-ATRP was initiated by pumping the CRM through the sensor cell at a speed of 70 mL h^{-1} (~2 min). The flow rate was then reduced to 2 mL h^{-1} after complete replacement of IRM with CRM. SI-ATRP was continued for ~60 min at ~23 °C and was monitored by QCM-D in real time. Polymerization was quenched by replacing CRM with IRM. Samples were then retrieved from the sensor cell, rinsed with methanol, and dried under a stream of nitrogen gas for further analysis.

III. RESULTS AND DISCUSSION

We first investigated experimental factors that could cause a change in the base line, including a change in pump speed and variation in flow over the sensor chip. In order to discriminate between these nonspecific effects from those caused by SI-ATRP, a gold-coated QCM-D chip modified with a SAM of (2) was mounted in the sensor chamber and primed with IRM, CRM, and IRM, as follows. After establishing a stable baseline with IRM, the flow rate was increased from 2 to 70 mL h^{-1} and then returned to 2 mL h^{-1} in less than 2 min. A sharp decrease in F and a sharp increase in D were observed as the flow rate was abruptly increased from 2 to 70 mL h^{-1} [marked as I in Fig. 2(a)], but both parameters in Fig. 2(a) reverted to their original baseline values as the flow rate was decreased to the original flow rate of 2 mL h^{-1}.

In another control experiment, shown in Fig. 2(b), IRM was flowed over a gold-coated QCM-D chip modified with a SAM of (2) for 20 min to obtain a stable base line. The peristaltic pump was then stopped briefly to switch the solution from IRM to CRM. Next, peristaltic flow of CRM was resumed at a speed of 70 mL h^{-1} until the exchange of IRM with CRM was completed (~2 min) and the flow rate was then gradually reduced to 2 mL h^{-1} and maintained at that flow rate for ~40 min. The same sequence was then repeated in reverse to switch CRM back to IRM and IRM was then flowed over the sensor for ~20 min at 2 mL h^{-1}. The change in the base line mirrored the changes observed in the initial sequence [Figs. 2(b) and 2(d)]. The data in Fig. 2(b) also clearly show that the final steady state value of ΔD are experimentally indistinguishable from the initial baseline, while the final steady state value of $\Delta F/n$ display a small, ~4 Hz offset from the initial base line values.

As the gold QCM chip used in this experiment was modified with a SAM of (2) that did not present any ATRP initiators at the surface, there was no polymerization upon introduction of CRM. Therefore, the changes in the baseline observed in Figs. 2(a) and 2(b) were solely due to changes in the flow rate and solution exchange. Furthermore, these changes are small enough to justify ignoring their contribution in the analysis of the kinetic profiles of SI-ATRP for SAMs that present immobilized ATRP initiator on their surface.

Figure 2(c) shows a QCM-D profile for a typical run of SI-ATRP of OEGMA from a pure, 100% SAM of (1). The black and red curves correspond to the frequency (F) and dissipation (D) change respectively, as a function of time. There are two regions in these plots, region I: a transient region in which IRM is replaced by CRM and a similar region in which CRM is switched back to IRM and region II: the linear region. In the linear region, a linear decrease in F as well as a linear increase in D was observed with time, presumably due to polymer growth. The molecular origin of this linear response is explored in more detail in the modeling section (*vide infra*). When CRM was then replaced with IRM, both F and D quickly reached a steady state, indicating termination of polymer growth. It is also notable that the change in F and D were perfectly synchronized in time.

We next studied the effect of initiator density on SI-ATRP of OEGMA [Figs. 2(d) and 2(e)]. By using mixed SAMs, it was possible to systematically change the ratio of (1) and (2) on the surface of the QCM chips. The slope of ΔF [Fig. 2(d)] and ΔD [Fig. 2(e)] as a function of time were found to be dependent on the surface density of the ATRP initiator (Table I), which had been previously measured by x-ray photoelectron spectroscopy (XPS) for these mixed SAMs of (1) and

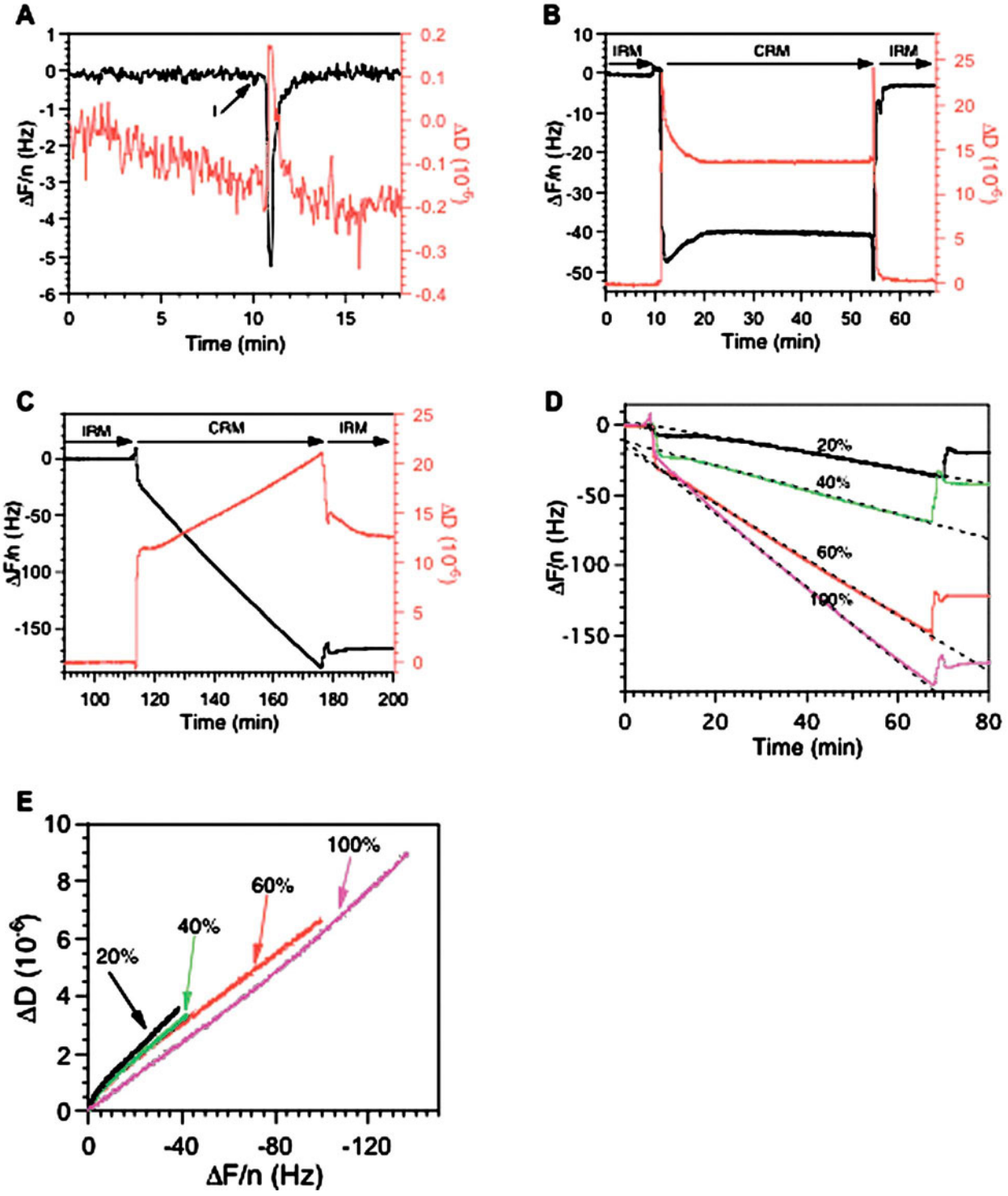

FIG. 2. Factors that cause baseline change (overtone $n=3$). Black and red curves represent frequency (F) and dissipation (D) change, respectively. ΔF is plotted in black and ΔD is plotted in red. (a) Pump speed change from 2 to 70 mL h^{-1} and back again caused a base line shift (I indicates onset of change of pump speed), which reverted to its original position as the flow rate returned to 2 mL h^{-1}. (b) A QCM chip was modified with a SAM of (2), and the solution was switched from IRM to CRM, and back to IRM over a 60 min period to determine the instrument baseline shift. (c) and (d) QCM-D recording of SI-ATRP of OEGMA (overtone $n=3$). A typical run of SI-ATRP from a gold-coated QCM-D chip functionalized with a pure SAM of (1) is shown in (c) and from the surface of four different mixed SAMs of (1) and (2) in (d). The black and red curves in panel (c) represent frequency (F) and dissipation (D) change, respectively, as a function of time. The different colored lines in (d) represent QCM-D chips prepared from mixed SAMs with a different solution mole fraction of (1): 20% (black), 40% (green), 60% (red), and 100% (magenta). The slope of ΔF against time in (d) was proportional to the solution mole fraction of (1) suggesting a dependence on the initiator density at the surface. (e) ΔD plotted against $\Delta F/n$ for SI-TRP of OEGMA from chips prepared from four different mixed SAMs of (1) and (2).

TABLE I. Impact of initiator density on frequency change measured by QCM-D.

Initiator (I)[a]	20%	40%	60%	100%
χ_1[b]	0.05	0.1	0.28	1
$K_F(I)$[c]	−0.56	−0.87	−2.0	−2.63

[a]Initiator percentage of total concentration [(1) and (2)] of thiol solution.
[b]Final surface ratio of initiator of mixed SAM of (1) and (2) as determined by XPS [Ref. 10].
[c]Slope of F decrease against time (between 20 and 60 min).

TABLE II. Material properties used in analytical model from Ref. 13.

Property	Value
Density (ρ_q)	2645 kg m^{-3}
Density (ρ_p)	1000 kg m^{-3}
Density (ρ_f)	1000 kg m^{-3}
Thickness (h_q)	3.325×10^{-4} m
Shear Modulus (G_p)	1×10^{4} N m^{-2}
Viscosity (η_p)	1×10^{-2} Ns m^{-2}
Viscosity (η_f)	1×10^{-3} Ns m^{-2}

(2).[11] As the initiator surface density increased, the slope of ΔF against time became more negative [k_F(I), Table I] and the slope of ΔD against time became more positive, which indicated an increase in mass and energy dissipation, respectively, at any given time. The parameter $\Delta F/n$ is an overall measure of mass change coupled to oscillation, which includes the mass increase due to tethered polymer chain growth as well as entrapped solvent.[12] From Fig. 2(b), we empirically define Eq. (1) to relate $\Delta F/n$ to polymerization time that fits the data well:

$$\frac{\Delta F}{n} = k_F(I) \times \text{time}, \tag{1}$$

where $\Delta F/n$ is the frequency change; $k_F(I)$ is an effective lumped reaction constant that is itself a function of the initiator surface density.

We also plotted ΔD as a function of $(\Delta F/n)$ plot for poly(OEGMA) grown from chips of different initiator density. When ΔD is plotted against $\Delta F/n$ [Fig. 2(e)], the time dependence of the system is removed, and we suggest that the physical significance of this plot is that it is a composite time-independent structural property of the system. The slope of ΔD vs $\Delta F/n$ decreased as the initiator density increased. This is in agreement with the fact that a denser initiator layer leads to a denser poly(OEGMA) film on the surface; a denser film is likely to be more rigid and hence exhibit less energy dissipation. Thus, unlike the slope of ΔF/time and ΔD/time, $\Delta D/(\Delta F/n)$ can be used as a viscoelastic signature of the interface.

Modeling of QCM-D results

In this section we show that the linear change in F and D that was experimentally observed as a function of polymerization time and for different initiator densities can be predicted from a continuum model.[13] In the limiting case of a viscoelastic layer in bulk Newtonian liquid whereby $h_p k_p \ll 1$ and $h_p \alpha_p \ll 1$, the change in resonant frequency (ΔF) and dissipation (ΔD) can be approximated as follows:

$$\Delta F \approx -\frac{1}{2\pi\rho_q h_q}\left[\frac{\eta_f}{\delta_f} + h_p\rho_p\omega - 2h_p\left(\frac{\eta_f}{\delta_f}\right)^2\frac{\eta_p\omega^2}{G_p^2+\omega^2\eta_p^2}\right] \tag{2}$$

and

$$\Delta D \approx -\frac{1}{2\pi f\rho_q h_q}\left[\frac{\eta_f}{\delta_f} + 2h_p\left(\frac{\eta_f}{\delta_f}\right)^2\frac{G_p\omega}{G_p^2+\omega^2\eta_p^2}\right), \tag{3}$$

where

$$\alpha = \frac{1}{\delta}\sqrt{\frac{\sqrt{1+\chi^2}-\chi}{1+\chi^2}}, \tag{4}$$

$$k = \frac{1}{\delta}\frac{\sqrt{\sqrt{1+\chi^2}}+\chi}{1+\chi^2}, \tag{5}$$

$$\chi = \frac{G}{\eta\omega}, \tag{6}$$

$$\delta = \sqrt{\frac{2\eta}{\rho\omega}}. \tag{7}$$

G is the elastic shear modulus, η is the shear viscosity of the polymer film, ω is the circular frequency, ρ is density, h is thickness, and the subscripts f, q, and p reference the fluid, quartz crystal, and polymer film, respectively. The change in frequency and dissipation are clearly a function of the bulk fluid term (η_f/δ_f), and terms that vary proportionally to the thickness of the polymer (h_p). For a given frequency of oscillation and known properties of the material, the change in frequency and dissipation are linearly proportional to the change in thickness (The change in frequency decreases as a function of thickness, and the change in dissipation increases as a function of thickness for $h_p k_p \ll 1$ and $h_p \alpha_p \ll 1$.) For a constant surface area, the linear increase in polymer thickness yields a linear increase in mass for a given density.

The material properties of the polymer tested here are unknown, so the following analysis is based upon the assumed material properties detailed in Table II (consistent with Voiniva *et al.*[13] Thus, the analytical results can be compared to the experimental results to qualify trends in the response, but do not provide parameters that can be quantitatively validated experimentally. The results plotted in Figs. 3(a) and 3(b) were generated with Eqs. (2) and (3). In the experimental results, the initiator density was varied between 20% and 100%, and for the analytical results, the polymer density and shear modulus were assumed to vary in the same proportion. As indicated in Fig. 3(a), the slope of the change in frequency as a function of polymer thickness varies linearly, and the trends observed are consistent with the *in situ*

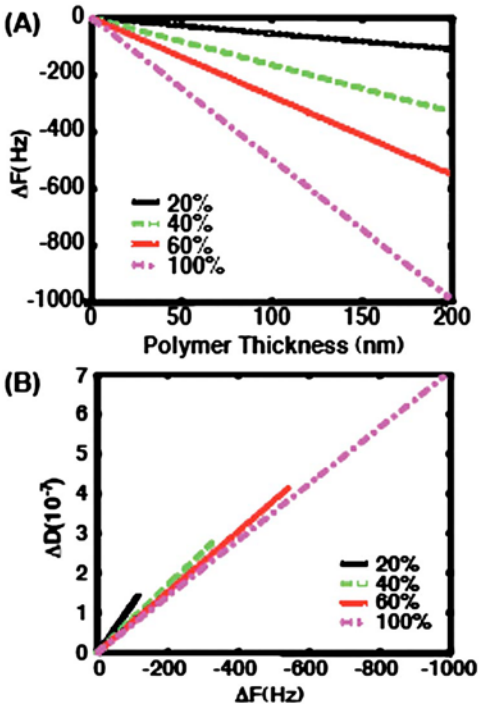

FIG. 3. Analytical prediction of changes in resonant frequency and dissipation as a function of polymer thickness for different initiator density: (a) change in resonant frequency as a function of polymer thickness and (b) change in dissipation plotted against change in resonant frequency for a given polymer thickness and varying initiator densities.

experimental measures presented in Fig. 2(d). The change in frequency is plotted against the change in dissipation at the corresponding polymer thickness in Fig. 3(b) for the analytical results. The result is a linear variation as well, which is intuitive since both F and D vary linearly with polymer thickness. Since the magnitudes of the slopes which correspond to the change in frequency and dissipation are smaller for corresponding smaller percentage of initiator density, the length of the lines representing the analytical data decrease with decreasing percentage of initiator density. These analytical results plotted in Fig. 3(b) qualitatively capture the trends in experimental results presented in Fig. 2(e). There is some discrepancy in the analytical and experimental results when the polymer thickness is $<\sim 3$ nm, but this may be the result of assumptions made in the continuum model (bulk material properties) which do not accurately capture the physics for layers $<\sim 3$ nm.

In summary, we have demonstrated that QCM-D is a unique tool to obtain time-resolved information about the kinetics of SI-ATRP. We believe that QCM-D is a powerful addition to the family of surface spectroscopy's that can directly report on the kinetics of overlayer deposition at the solid-liquid interface by providing a direct, quantitative measure of the amount, and the viscoelastic properties of the deposited overlayer.

ACKNOWLEDGMENTS

The authors thank Dr. Janos Vörös, Fernanda Rossetti, and Laurent Feuz for helpful discussion. H.M. is grateful for a fellowship from the Center for Biologically Inspired Materials and Material Systems (CBIMMS) and the Graduate School at Duke University. This work was supported by the CDC through NCID R01 CI-00097 to A.C.

[1] J. Pyun, T. Kowalewski, and K. Matyjaszewski, Macromol. Rapid Commun. **24**, 1043 (2003).
[2] *Polymer Brushes: Synthesis, Characterization, Applications*, edited by R. C. Advincula, W. J. Brittain, K. C. Caster, and J. Ruhe (Wiley-VCH, Weinheim, 2004).
[3] G. K. Jennings and E. L. Brantley, Adv. Mater. (Weinheim, Ger.) **16**, 1983 (2004).
[4] S. Edmondson, V. L. Osborne, and W. T. S. Huck, Chem. Soc. Rev. **33**, 14 (2004).
[5] D. J. Li, X. Sheng, and B. Zhao, J. Am. Chem. Soc. **127**, 6248 (2005).
[6] O. Prucker and J. Ruhe, Macromolecules **31**, 602 (1998).
[7] F. Hook, A. Ray, B. Norden, and B. Kasemo, Langmuir **17**, 8305 (2001).
[8] M. Rodahl, F. Hook, and B. Kasemo, Anal. Chem. **68**, 2219 (1996).
[9] M. Rodahl, F. Hook, A. Krozer, P. Brzezinski, and B. Kasemo, Rev. Sci. Instrum. **66**, 3924 (1995).
[10] H. Ma, M. Wells, T. P. Beebe, Jr., and A. Chilkoti, Adv. Funct. Mater. **16**, 640 (2005).
[11] H. Ma, J. Hyun, P. Stiller, and A. Chilkoti, Adv. Funct. Mater. **16**, 338 (2004).
[12] F. Hook, B. Kasemo, T. Nylander, C. Fant, K. Sott, and H. Elwing, Anal. Chem. **73**, 5796 (2001).
[13] M. V. Voinova, M. Rodahl, M. Jonson, and B. Kasemo, Phys. Scr. **59**, 391 (1999).